Hybrid Advances 7 (2024) 100292

Contents lists available at ScienceDirect

Hybrid Advances

journal homepage: www.journals.elsevier.com/hybrid-advances

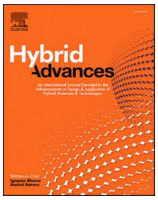

Review Article

Recent advances in metal oxide-biochar composites for water and soil remediation: A review

Hermann Tamaguelon Dzoujo [a], Victor Odhiambo Shikuku [b,*], Sylvain Tome [a], Aurelle Clandy Ntinkam Simo [a], Emily C. Ng'eno [b], Zachary M. Getenga [c], Marie Annie Etoh [a], David Daniel Joh Dina [a]

[a] Department of Chemistry, Faculty of Sciences, University of Douala, P.O. Box 24157, Douala, Cameroon
[b] Department of Physical Sciences, Kaimosi Friends University, P.O. Box 385, 50309 Kaimosi-Kenya
[c] Department of Physical Sciences, Machakos University, P.O. Box 136, 90100, Machakos-Kenya

ARTICLE INFO

Keywords:
Environmental applications
Functionalization
Physicochemical properties
Metal/biochar composites
Metal oxides

ABSTRACT

During the last decades, biochar (BC) has proven to be an innovative candidate in various environmental applications. Nevertheless, the use of biochar in improving soil fertility, immobilizing contaminants and treating wastewater has presented many limitations. Nanomaterial technology has been used to improve the physicochemical properties of biochars, including emerging methods such as chemical precipitation, direct pyrolysis and impregnation of biochars with metals (Fe, Zn, Ce, Cu, Zr, Ti etc) or their oxides. This review discusses recent advancements on the potential, limitations, and prospects of using metal-biochar composites for wastewater treatments and soil remediation. Functionalization of biochar with metal oxides can exacerbate the specific surface area up to 98 %, and diminish the porosity structure up to 89 %. The performance of these metal-biochar composites, which depends on the raw material/precursor of the biochar, the identity of the metal/guest ion, the preparation conditions and the activation method, has shown that the removal rates for inorganic and organic contaminants in the aqueous phase vary from 80.5 to 100 % and from 52.90 to 100 % respectively and that the immobilization rates for heavy metals in soils vary from 16 to 100 %. Remediation mechanisms for various adsorbates in aqueous media and soils generally include electrostatic attraction, oxidation/reduction, complexation and precipitation. Life cycle assessment (LCA), pilot-scale, cost analysis, potential environmental risks, and machine learning modelling studies are found to be lacking for metal-biochar composites and provide areas for future research.

1. Introduction

Access to clean and safe water at all times is a fundamental human right. The sustenance of life on earth is dependent on the quality and quantity of water, and it has been argued that water is life. However, the increased industrialization at the turn of the twentieth century has not only been beneficial to the human race but has also been accompanied by increased levels of pollution and stress in access to clean water. These industrial processes result in the release of effluents or wastewater laden with organic and inorganic chemicals that endanger human, animal, and aquatic life. In the developing world, where a large fraction of the population is not connected to centralized water treatment facilities and therefore depends on rivers, lakes, and groundwater, water pollution is a serious threat that requires immediate action [1]. Ad hoc and unscientific disposal of agro and industrial chemicals such as dyes, pharmaceutical compounds, detergents, personal care products, and emerging contaminants among others are among the main sources of water contamination. Because chemicals have been associated with various disorders and toxicological effects in both human and aquatic life, their occurrence in water resources is of great environmental concern, even at low concentrations [1,2]. Environmental and water resource management authorities around the world have passed increasingly strict drinking water quality regulations as a result of these concerns. Unfortunately, most emerging chemical pollutants are resistant to standard water treatment methods such as flocculation and coagulation [3]. Although emerging technologies such as membrane filtration and chemical treatment are effective in removing most contaminants from water, they typically require large capital investments

---

* Corresponding author.
E-mail address: vshikuku@kafu.ac.ke (V.O. Shikuku).

https://doi.org/10.1016/j.hybadv.2024.100292
Received 20 July 2024; Received in revised form 20 September 2024; Accepted 20 September 2024

and have significant operating costs, which prevents them from being broadly adopted, especially in emerging economies [4]. Scientists are continually researching low-cost, efficient, and sustainable technologies (materials and processes) to produce potable drinking water [3]. Some of the low-cost materials include geopolymers [5–9], natural zeolites [10], clays [11], activated carbons derived from biomass [12,13], diatomaceous earth [14] and biochars [15,16]. Biochars have received considerable attention because of the relatively low preparation costs and availability of a plethora of waste biomass that provides ready feedstock. Biochar is a carbonaceous biomaterial derived from the thermal degradation by pyrolysis of biomass waste in aerobic and anaerobic environments [17,18]. It is an excellent adsorbent for the remediation of contaminants in water and soil [19–22] due to its specific chemical properties, such as alkalinity, aromaticity and important textural properties [23]. Furthermore, the remediation mechanism by ion exchange and complexation between biochar and water or soil pollutants remains limited due to the low density of surface chemical functions. However, the functionalization of biochar can include treatment with acid, alkali, oxidizing agents and metal salts to increase the specific surface area and enrich the surface of the biochar with oxygenated groups in the composite compared with pristine biochar [24]. In recent decades, metal/biochar composites have been functionally superior to pristine biochars due to the synergy between the properties of guest and host materials and environmentally benign materials for water treatment. They have been applied as adsorbents for the sequestration of water pollutants and soil remediation. However, a synthesis of existing literature on the recent developments in the use of metal-biochar composites for environmental remediation is lacking. Therefore, this study will focus on the gaps in understanding the synthesis, characteristics and use of metal biochar composites in the remediation of pollutants in water and soil, by re-evaluating recently (2009–2023) peer-reviewed and published literature from different scientific databases (PubMed and Google Scholar), and literature repositories (Research Gate). This review describes in detail the synthesis of metal/biochar composites and their application as adsorbents in the removal of toxic and recalcitrant heavy metals and organic micropollutants such as dyes from water. The interaction mechanisms between this class of composite materials and various contaminants are also discussed in detail. The use of this category of materials for soil remediation is also presented. Metal/biochar composites, like other adsorbents, are not without limitations. The inherent limitations, gaps, and opportunities for further investigations are also presented. A concise synthesis and summary of recent literature on metal-biochar composites for water and soil remediation is the novelty of the present work.

2. General characteristics of biochar

Biochar is a material made up mainly of carbon resulting from the pyrolysis of biomass in aerobic or anaerobic conditions [25]. BC is generally used in power generation and the treatment of contaminants (Fig. 1) due to these intrinsic and extrinsic characteristics [26]. The chemical composition of the biochar composite (BC) is controlled by the choice of the feedstock and the pyrolysis conditions such as pyrolysis temperatures, reaction intervals, and burning rate, thus conferring to the final product a large specific surface area, well-developed porosity structure, and various functional group that govern reaction mechanism and performance. For example, previous work (Table 1) shows that the hydrogen-to-carbon mass (H/C) and oxygen-to-carbon (O/C) ratios decrease with increasing pyrolysis temperatures, resulting in an increase in the aromatic compound content and good stability of the carbon skeleton. Mohammed et al. [27], Kameyama et al. [28] reported that the specific surface area and the porosity increased significantly with increasing heating rate and pyrolysis temperature. It has been shown that, at relatively low temperatures (200–400 °C), the developed biochar has more oxygen-rich surface functional groups, including carboxyl-COOH, phenolic-OH, and –CHO groups due to dehydration accompanied by modification of the plant biomass, which improves immobilization and binding efficiency with pollutants. On the other hand, at higher temperatures (>400 °C), progressive polymerization, loss of functional groups, dehydrogenation, decreased ion exchange capacity, and pore closure were observed, making the biochar produced less effective in environmental remediation [29]. Over time, the association of metal oxides/non-metals with biochar, resulting in metal-biochar composites, has emerged as a facile and techno-economic technique approach for improving the properties of pristine biochars and their composites [30].

3. Synthesis of metal-biochar composite

Metal-biochar composites have been developed because of the limitation of pure biochar in environmental remediation and to obtain new materials that exploit the properties of adjuvant and biochar. Table 2 gives a general overview of the various methods of preparing metal-biochar composites, together with their advantages. The synthesis of metal-biochar composite includes impregnation of biomass with metal salts, chemical precipitation, direct pyrolysis, and other emerging methods (Fig. 2). Depending on the reagents used and the preparation conditions, nano-scale magnetically responsive biochar composites be obtained.

Fig. 1. Application of biochar in environmental remediation.

Table 1
Some physicochemical characteristics of biochars.

Feedstock	T(°C)	Total pore volume cm^3g^{-1}	Specific Surface area m^2g^{-1}	H/C	O/C	References
Orange peel	200–500	0.01–0.02	7.75–42.40	1.14–0.38	0.45–0.21	[20]
Peanut shell	300–700	ND-0.20	3.14–448.20	0.67–0.25	0.29–0.12	[31]
Pineal shell	350–550	0.001–0.038	0.82–228.11	0.06–0.04	0.32–0.15	[27]
Alfalfa	350–650	ND	3.50–183.00	0.80–0.20	0.20–010	[28]
Domestic wastewater sludge	400	ND	ND	0.08	0.19	[28]
Timothy grass	450	ND	179	0.03	0.42	[32]
Municipal sewage sludge	500–900	0.056–0.099	25.42–67.60	0.09–0.08	0.45–0.12	[33]
Turkey litter	700–800	ND	21.8	0.05	0.28	[34]
Walnut shell	900	ND	227.1	0.02	0.03	[34]

Table 2
Various methods for obtaining metal-biochar composites.

Modification methods	Pyrolysis temperature (°C)	Advantageous characteristics generated	References
$KMnO_4$-modified biochar	550	Introduction of a large number of acid functional groups on the surface of the BC	[35]
$Cu(NO_3)_2$-modified biochar (Cu-BC)	450	Enhanced electrostatic and complexation interactions during adsorption	[36]
Biochar modified with Fe(III) (Fe-BC)	–	Increased performance with the addition of FeOH sites and $FeOH_2^+$ to the surface of the BC	[37]
MnOx-modified biochar (MnOx-BC)	400	Increased specific surface area of composites	[38]
MgO-modified biochar (MgO-BC)	600	Production of a highly mesoporous material	[39]
Biochar modified with TiO_2 (TiO_2-BC)	ND	Photogeneration of electrons due to interactions between BC and TiO_2	[40]
Biochar modified with ZnO (ZnO-BC)	600	Surface enlargement and reinforcement of the positive charge of the resulting composite.	[41]
Biochar modified with ZrO_2 (ZrO_2-BC)	ND	Improving sonocatalytic activity by adding ZrO_2 to the biochar matrix	[42]
Biochar modified with CeO_2 (CeO_2-BC)	500	Improving sonocatalytic activity by adding CeO_2 to the biochar matrix	[43]

3.1. *Synthesis of BC-magnetic composites*

Table 3 summarizes the methods used to prepare magnetized biochar. Common methods for preparing BC magnetic composites (MBC) are generally liquid phase precipitation, which requires preparing BC first, then mixing the BC with Fe^{3+}/Fe^{2+} ions and the magnetic oxide precipitated by the dropwise addition of strong alkali NaOH/NH_4OH into the mixture. This method provides a better distribution of nanoparticles on the surface of the biochar but can generate impurities when the resulting material is applied [44]. Impregnation involves immersion

Table 3
Magnetic biochar synthesis process.

Preparation methods	type of synthesis	Types of biochar composites produced	References
1) Pyrolysis of feedstock pre-treated with $FeCl_3$	Impregnation technique	ZVI-BC and γFe_2O_3-BC	[46]
2) Addition of the biomass to a solution containing ferrous chloride and ferric chloride, then addition of a NaOH solution to raise the pH to 10, centrifugation of the suspension and pyrolysis.	Co-precipitation technique	Fe_2O_3-BC	[47]
3) The biochar and stainless steel bottles are agitated in a ball mill	Ball milling technique		[48]
4) Feedstock pre-treated with $MgCl_2$, $FeCl_3$ was treated by hydrothermal carbonization, and the pH was adjusted to 10 with a NaOH solution.	Hydrothermal technique	$MnFe_2O_4$-BC	[49]
5) BCs pretreated respectively with HCl, H_2O_2 and KOH introduced into a Fe(III) solution followed by reduction with $NaBH_4$ or KBH_4	Reduction technique	nZVI-HCl-BC, nZVI–H_2O_2–BC and nZVI-KOH-BC,	[50]

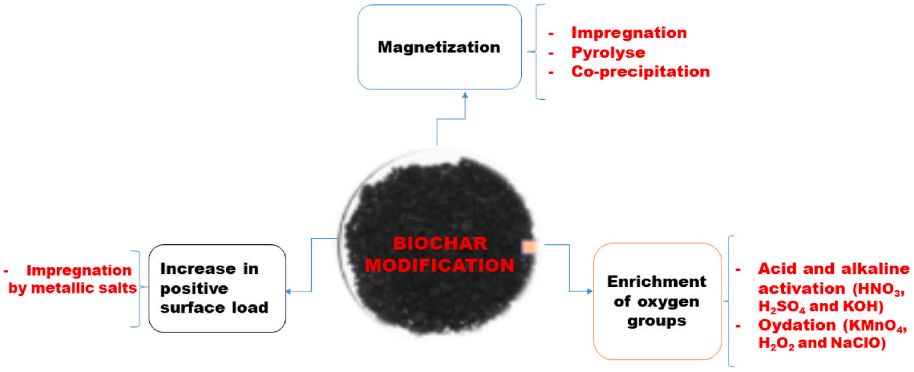

Fig. 2. Different types of biochar modifications depending on their characteristics.

of the biomass powder in the Fe^{3+}/Fe^{2+} solution or co-precipitating the Fe^{3+}/Fe^{2+} with chemicals before pyrolysis and the composite resulting from this synthesis technique is highly effective at binding heavy metals, but can also cause secondary pollution if it leaches [45]. Liquid phase reduction, which involves injecting a sodium or potassium borohydride solution ($NaBH_4/KBH_4$) into a mixed solution of BC and Fe^{3+}/Fe^{2+} under nitrogen purging to reduce Fe^{3+}/Fe^{2+} to Fe^0. It allows smaller metal particles to be distributed on the surface of the biochar but is limited by the toxicity and high cost of the chemical reducers used. Ball milling is a widely used method for producing MBC composites on a large scale, as it produces materials with a high specific surface area and rich acid functionality. However, this method requires a device with a large reservoir and a single function.

3.2. *Synthesis of nano-metal oxide/hydroxide BC*

The preparation of nano-metal oxide biochars (NMOBCs) is a promising process due to the incorporated nanomaterials that remarkably improve surface functional groups, creating new adsorption and catalytically reactive sites [20]. The process of preparation of nanoscale oxide/hydroxide-based biochar composites can be done by bio-accumulation of target elements, so the goal is the enrichment of the soil with the target element contained in the fertilizers during the planting of biomass that will make BC, after pyrolysis, rich in the target element. By pretreatment of biomass with metallic salts followed by pyrolysis, the resulting BC consists of nano-scale metal oxides fixated on both the surface and inside the carbonaceous material. By insertion of metal oxide nanoparticles after BC pyrolysis into the surface and internal pores of BC [51]. Fig. 3 illustrates different methods for the preparation of biochar-metal oxide nanocomposites.

4. Physicochemical properties of a metal-biochar composite

4.1. *Chemical properties*

Chemical properties of metal-biochar composites are defined by the point of zero charge (PZC), the cation exchange capacity (CEC), and the surface functional group density and distribution. For example, Wang et al. [53] showed that the adsorption of pb^{2+} on a MnO_2-biochar composite was maximal at pH (5.0) > pHpzc (3.2) due to the negative surface charge which favours electrostatic attraction and the cations Pb^{2+} or $PbOH^+$. On the other hand, maximum adsorption of Reactive Yellow 39 on the ZrO_2-biochar composite carrying a positive surface charge was favoured at pH (6.0) < PZC (7.35) [42]. Furthermore, it is reported in the literature [54] that the CEC of biochar ranges from 8 to 40,000 mmol/kg. Moreover, this can increase considerably when the biochar is modified by metal oxides.

The work of Rajapaksha et al. [55] reported that the chemical oxidation of biochar induces acidic sites such as phenolic, carboxylic and lactonic groups on the biochar surface at relatively low temperatures. Lawrinenko et al. [56] showed that BC prepared from biomass pre-treated with iron aluminum trichloride exhibited Al–*O*–C and Fe–*O*–C bonds in its structure. This promoted an extra distribution of metal atoms on the resulting BC. As an outcome, the resulting iron-biochar composites were favourable for the retention and encapsulation of heavy metals and organic contaminants through enhanced surface complexation, precipitation, and electrostatic interactions. In addition, Yang et al. [57] synthesized a g-MoS_2-coated biochar nanocomposite for ciprofloxacin (EDA) adsorption and the resulting composite provided more π-electrons compared to pristine biochar, thus enhancing the π-π EDA interactions. On the other hand, the ion exchange capacity can also increase with zero net charge point when the surface of the BC is coated with nanoscale oxide/hydroxide.

4.2. *Physical properties*

The physical properties of metal-biochar composites are directly related to biochar preparation conditions such as reactor temperature and residence time, the addition of oxygen-containing media in the process (air, pure oxygen, CO_2, and steam) and/or post-production processing to modify the final product that more or less significantly affects the textural properties, bulk density, pore size, and pore volume distribution of the resulting material [58]. Li et al. [59] synthesized corn-derived biochar modified with ZnO/ZnS. The ZnO/ZnS treatment improved the BET surface area of the composite from 102.9 to 397.4 m2/g compared with the unmodified biochar and allowed the nano ZnO/ZnS to be uniformly distributed over the surface of the BC. Shen et al.[60 [][][]synthesized an MgO-coated biochar for lead removal in the aqueous phase and reported that the specific surface area of the biochar was significantly improved from 0.07 to 26.56 m^2/g with MgO coating inducing a significant increase in the Pb removal rate from 23 % to 74 %. However, the type of biomass used and certain metal incorporation methods during the preparation of metal-biochar composites can critically affect their properties and structures. For example, co-precipitation, integrated adsorption-pyrolysis, and electric field-assisted pyrolysis are the commonly reported methods for

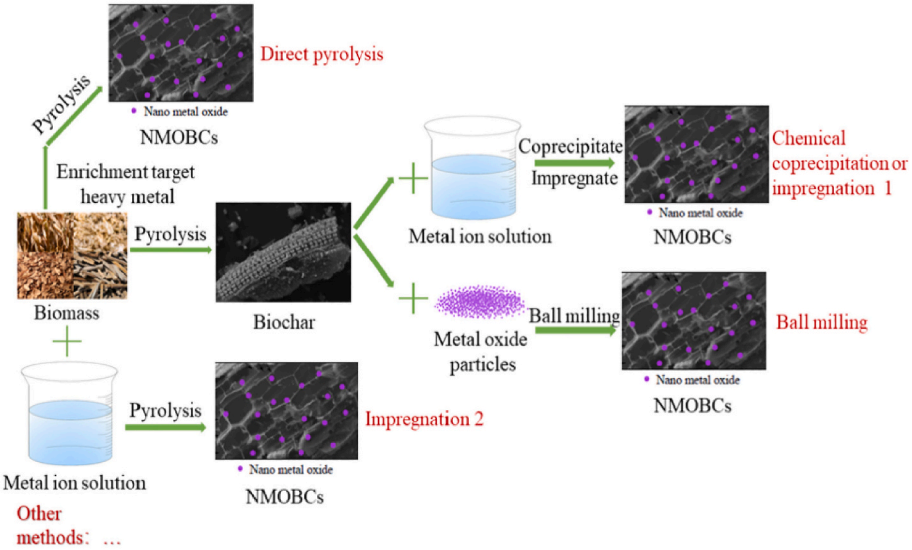

Fig. 3. Different approaches in the synthesis of nano-scale metal oxide loaded biochars. Reproduced with permission from Zhao et al. [52].

preparing oxide/hydroxide composites. Numerous studies have revealed that the integrated adsorption-pyrolysis approach method for the synthesis of Fe(III) oxide-biochar composite is significantly more beneficial than the post-precipitation approach of Fe(III) oxides in pristine biochar due to the distribution of the iron oxide particles in the carbon matrix, which results in a significant increase in surface area from 24.59 to 92.54 m^2/g [61]. On the other hand, the physical properties of the metal-biochar composite may decrease during the synthesis, because of the insertion of metal oxide nanoparticles within the pores, probably favouring an increase in the number of binding sites. Table 4 highlights the impact of the modification of the textural properties by various metal oxide nanoparticles on different biomass biochar. Unfortunately, there is no unified scientific theory for predicting trends in the textural properties of metal-biochar composites. Machine learning provides a powerful tool for the prediction of the textural properties of materials based on the characteristics of the feedstock and the synthesis conditions as input variables. However, machine learning-based research works for metal/biochar composites are lacking. As such, the textural properties of the metal/biochar properties must be determined experimentally.

5. Applications of metal oxide -biochar composite

The development of metallic oxide biochars has been subjected to research in areas such as environment, agriculture, and energy. Metal oxide-biochar composites are suitable, promising, and sustainable candidates for a wide range of environmental applications, including soil fertility improvement, contaminant immobilization, wastewater treatment, and in situ carbon sequestration [30]. Organic or inorganic contaminants are generally eliminated by adsorption or photocatalysis on biochar metal oxides and the retention mechanisms of these adsorbates include electrostatic attraction and complexation reactions, oxidative decomposition and reduction, etc. (Fig. 4). However, previous work (Tables 5 and 6) shows that the maximum adsorption capacities (Qm) of biochar metal oxide composites to inorganic and organic pollutants vary arbitrarily depending on the type of biomass and preparation conditions.

5.1. Removal of inorganic pollutants

The non-biodegradability of heavy metals leads to their accumulation in living beings through the food cycle. This accumulation can trigger serious health diseases such as cancer, endocrine disorders, etc. There exist different methods for ion exchange, precipitation, adsorption, complexation, electrostatic interaction, etc. which can be used for the efficient removal of heavy metals by metal-biochar [70]. For lead removal, the addition of 3.65 % Mn into a biochar matrix increased the Pb elimination percentage from 6.4 % to 98.9 % [53]. This was attributed to an increased degree of the hydroxyl group density and change in surface charge (pH_{PZC}). Furthermore, the Pb retention percentage and maximum adsorption density following the incorporation of Mn increased fivefold relative to the unmodified biochar. Furthermore, for the removal of U(VI), Li et al. [62] prepared $KMnO_4$ modified BC. The adsorption capacity of U (VI) increased via coordination and Lewis acid-base interaction, which is a result of the increase in functional groups containing oxygen. Tan et al. [71] for Hg (II) adsorption fabricated BC by modifying it with Na_2S and KOH. They showed that the modifications were responsible for the increased BET surface area from 32.85 to 55.58 m^2/g for the Na_2S BC treatment and to 59.23 m^2/g following KOH treatment with concomitant Hg (II) retention efficiencies of 32.12 % and 76.95 %, respectively. The improvement of the mercury removal rate by Na_2S BC could be due to the precipitation reaction between Na_2S on the surface of BC and Hg (II). Table 5 highlights the adsorption capacities of metal-biochar composites compared to unmodified biochar toward heavy metals. For example, for Cr (VI) removal, Zhang et al. [72] used magnetized biochar (MBC) and chitosan-modified biochar (CMBC). An increase in chromium retention capacities from 75.8 to 127 mg/g was observed for MBC and CMBC, respectively. The Cr (VI) adsorption performance of CMBC resulted respectively from electrostatic attraction (Fig. 5a), direct and indirect reduction (Fig. 5b and c), ion exchange (Fig. 5d and e), and chelation (Fig. 5f) between Cr (VI) and the C=C, OH, C–O, NH groups on the surface of CMBC.

5.2. Removal of organic contaminants

Organic compounds are often found in wastewater. Among these organic compounds dyes, pesticides, phenol, and antibiotics, because of their toxicity, complex aromatic structure, and non-biodegrability, are being given more attention. Table 6 is an illustration of the relative adsorption densities of metal-biochar composites reported for the remediation of organic pollutants. For example, Liu et al. [82] removed tetracycline (TC) using BC modified by chitosan and FeSx. This pre-treatment increased the maximum adsorption capacity for TC from 51.78 to 193.01 mg/g. The mechanism entailed pore filling, electrostatic interactions, chelation and π-π stacking as shown in Fig. 6. Elsewhere, Eltaweil et al. [63] have prepared a magnetic biochar (nZVI/BC) for the abatement of Malachite green. They found that magnetising the biochar resulted in an 82 % increase in specific surface area for a maximum sequestration capacity of 515 mg/g induced by the oxidation and reduction of nZVI.

To remove phenol by photocatalytic degradation in water, Lisowski et al. [83] used ultrasound-assisted methodology to prepare TiO_2-BC. The phenol degradation rate by UV-coupled TiO_2-BC reached 64.1 %

Table 4
Physical properties of Biochar (BC) and metal-biochar composites.

Biomass	Modification method	Specific Surface area (BC) m^2g^{-1}	Specific surface area (Modified BC) m^2g^{-1}	Total pore volume (BC) cm^3g^{-1}	Total pore volume (ModifiedBC) cm^3g^{-1}	References
Ficus microcarpa aerial root	MnO_2	686	284	0.95	0.35	[62]
Corn straw	nZVI	44	80.10	0.13	ND	[63]
Corn straw	$MnFe_2O_4$	2.68	38.05	ND	ND	[64]
Corncob	MgO	0.07	26.56	ND	ND	[60]
Leaf litter	CeO_2, MoS_2 and magnetic	89.4	127.6	0.032	0.087	[65]
Peanut hull	Zero valent iron	359.80	8.81	0.45	0.05	[66]
sugarcane harvest residue (SHR)	Fe(III) oxides	24.59	92.54	0.038	0.101	[67]
Pinus massoniana	Manganese-oxide	369	361	0.200	0.194	[53]
corn stover	ZnO/ZnS	102.9	397.4	ND	ND	[59]
Corn straw	Ferromanganese binary oxide	61.90	71.64	0.036	0.114	[68]
Rice husk	MnO_x	234.8	430.2	0.101	0.092	[69]

ND: not determined.

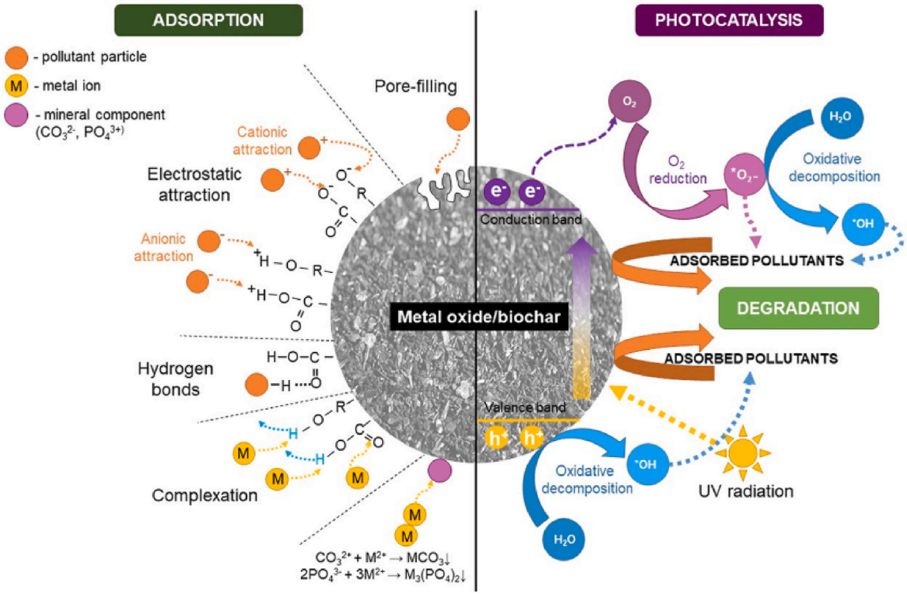

Fig. 4. Degradation processes of organic and inorganic adsorbates on the surface of metal-oxide-biochar composites. Reproduced with permission from Weidner et al. [19].

Table 5
Adsorption capacities of biochar-metal composites for the elimination of inorganic pollutants in aqueous solution.

Biomass	Modification method	Adsorbates	Q_e (mg/g)	Q_m (mg/g)	% Removal	References
bamboo residues	Magnetic and Chitosan	Cr(VI)	ND	75.80 and 127	90.0	[72]
Peanut hull	Zero valent iron	Cr (VI)	ND	223.20	100.0	[66]
Water hyacinth	Graphene oxide	Cr (VI)	47.80	150.00	95.6	[73]
Pinus massoniana	Manganese-oxide	Pb (II)	91.70	121.80	98.9	[53]
Carbonaceous biomass	ZnS and magnetic	Pb (II)	262.40	367.70	100.0	[74]
Corn straw	$MnFe_2O_4$	Pb (II)	80.40	154.94	99.0	[64]
Leaf litter	CeO_2, MoS_2 and magnetic	Pb (II)	24.90	263.60	99.6	[65]
Rice husk	MnO_x	Pb (II)	60.70	86.50	ND	[69]
Rice husk	3D MnO_2	Pb (II)	16.02	70.90	80.5	[75]
Rice husk	hydroxyapatite	Pb (II)	ND	110.20	≥99.5	[76]
Ficus microcarpa aerial root	MnO_2	U (VI)	ND	24.60	82.0	[62]
Lufa cylindrical fiber	MnO_2	U (VI)	ND	904.00	100.0	[67]
Corn straw	Ferromanganese binary oxide	Cd (II)	100.0	101.00	ND	[68]
Straw	Fe–Mn oxide	Cd (II)	ND	131.03	ND	[77]
Rice husk	3D MnO_2	Cd (II)	8.84	84.76	92.1	[75]
Rice husk	hydroxyapatite	Cd (II)	ND	88.10	≥99.5	[76]
Raw corn	TiO_2	Cd (II)	ND	72.6	70	[78]
Corn straw	Na_2S	Hg (II)	3.23	5.11	76.95	[71]
Straw	Fe–Mn oxide	Hg (II)	ND	86.82	ND	[77]
Corn stover	ZnO/ZnS	Cu (II)	27.05	91.20	38.98	[59]
Corn straw	Ferromanganese binary oxide	Cu (II)	71.40	64.90	ND	[68]
Corn straw	MnO_x	Cu (II)	19.60	160.00	ND	[38]
Municipal solid waste	KOH	As (V)	33.20	31.0	100.0	[79]
Rice husk	Ternary HA/Fe–Mn oxides	As (V)	0.00	35.59	ND	[80]
Rice residue	$Zr(OH)_4$–Fe_3O_4-Biochar	As (V)	ND	40.80	ND	[81]

ND: not determined, Qe: equilibrium adsorption capacity, Qm: maximum adsorption capacity.

and 33.6 %, respectively, which, exceeded the performance of pristine biochar consistent with the increased BET surface area following impregnation with TiO_2 and expanded porosity structure. Additionally, the inclusion of TiO_2 ameliorated the visible light absorption capacity necessary for photocatalytic degradation. The composite was recyclable with reuse of up to 5 cycles before substantial loss of reactivity. Thus, the TiO_2-BC prepared by this method had good cycle stability and high photocatalytic efficiency. Fig. 7 describes the mechanisms for the removal of phenol using a zinc oxide-modified biochar composite [84]. The paper, printing, and textile industries make extensive use of dyes, which are a group of organic contaminants. Recently, Rubangakene et al. [85] prepared green pea biochar (GPBC) and nano ferromagnetic green pea biochar (NFGPBC) by the ferrous/ferric coprecipitation synthesis method to remove methylene blue in aqueous solution. They showed that GPBC and NFGPBC had BET surface areas of 372.54, and 147.88 m^2g^{-1}, and the corresponding maximum adsorption capacities (Qm) of 217.40, and 175.44 mg/g, respectively. The decrease in NFGPBC adsorption performance was attributed to the agglomeration of iron particles on the biochar surface. On the other hand, recycling and reuse of the synthesized GPBC and NFGPBC materials performed over five adsorption cycles revealed that NFGPBC demonstrated excellent cyclic performance by achieving a minimum loss of 8.9 % of capacity due to paramagnetic properties. Lu et al. [86] fabricated TiO_2-biochar for the removal of methyl orange (MO). They revealed that TiO_2-BC possessed a high degradation catalytic activity in MO (98.88 % of the percentage of decolourization and 83.23 % of the mineralization rate).

Table 6
Adsorption capacities of biochar-metal composites for the elimination of organic pollutants in aqueous solution.

Precursor	Pre-treatment method	Adsorbates	Q_e (mg/g)	Q_m (mg/g)	% Removal	References
municipal waste sludge	Chitosan and Fe/S	Tetracycline	51.78	193.01	ND	[82]
Hazelnut shell	zero-valent iron	Tetracycline	ND	39.10	96.6	[88]
Orange peels	$LaCl_3$	Tetracycline	ND	143.20	ND	[89]
Camphor tree leaves	ZnO	Ciprofloxacin	ND	449.4	ND	[90]
Potato haulm	MnOx	Ciprofloxacin	ND	8.37	ND	[91]
Palm kernel	Magnetic	Phenol	3.20	10.84	52.9	[92]
Rice husk	S-nZVI	Nitrobenzene	550.00	588.20	100.0	[93]
Corn straw	nZVI	Malachite green	ND	515.77	99.9	[63]
Bamboo	$TiO_2/MgO/ZnO$	Methylene blue	15.80	62.50	ND	[94]
Green pea peels	Nano-ferromagnetic	Methylene blue	217.40	175.44	ND	[85]
Waste walnut shell	TiO_2	Methyl orange	77.5	ND	98.88	[86]
Paper and pulp sludge	Fe_2O_3	Methyl orange	22.00	46.60	52.79	[45]
Macroalgae	Fe_2O_3	Acid orange 7	ND	382	ND	[95]

ND: not determined, Qe: equilibrium adsorption capacity, Qm: maximum adsorption capacity.

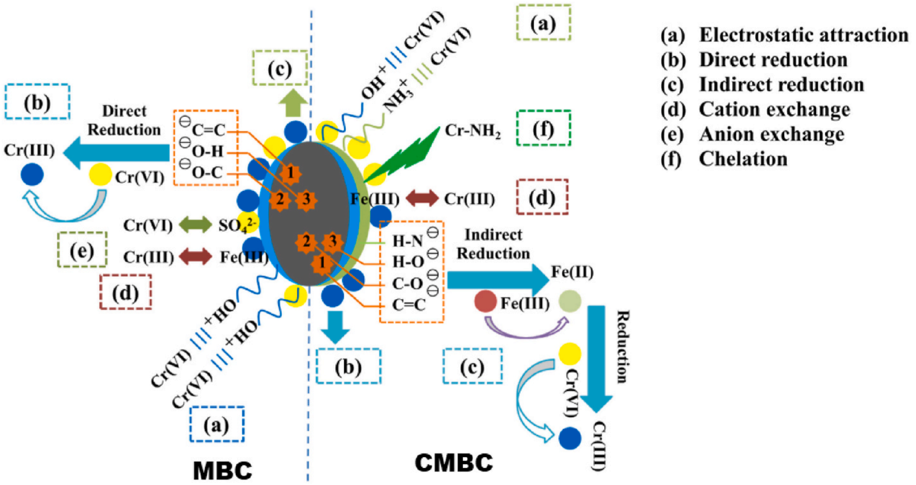

Fig. 5. Mechanisms of Cr (VI) sequestration onto metal-biochar composite. Reproduced with permission from Zhang et al. [72].

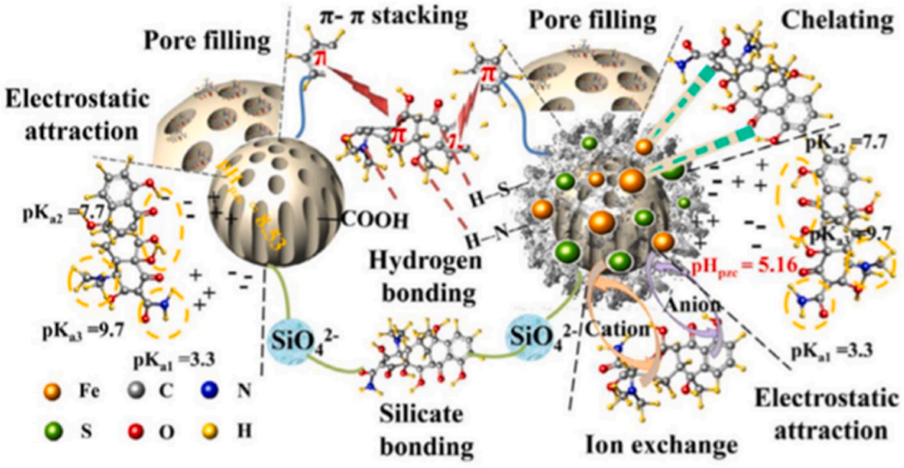

Fig. 6. The tetracycline binding mechanism onto metal-biochar composite. Reproduced with permission from Liu et al. [82].

After 5 cycles of repeated use, the TiO_2-BC catalyst still exhibited a high activity towards MO degradation, where the decolourization efficiency and the MO mineralization efficiency reached 92.45 % and 76.56 % for a negligible loss of activity. Khataee et al. [87] also described the ultrasonically catalytic mineralization of reactive blue 69 (RB69) by TiO_2-loaded biochar. They showed that the retention rate of RB69 by ultrasound/TiO_2-BC was higher than that of ultrasound/BC (that is, 98.1 % and 63.8 %, respectively). The presence of TiO_2 increased the density of potential reactive sites on the solid surface and promoted the obtaining of –OH, radicals associated with the cracking of water molecules. In addition, the degradation efficiency of TiO_2-BC was still 92.1 % after 5 cycles of reuse.

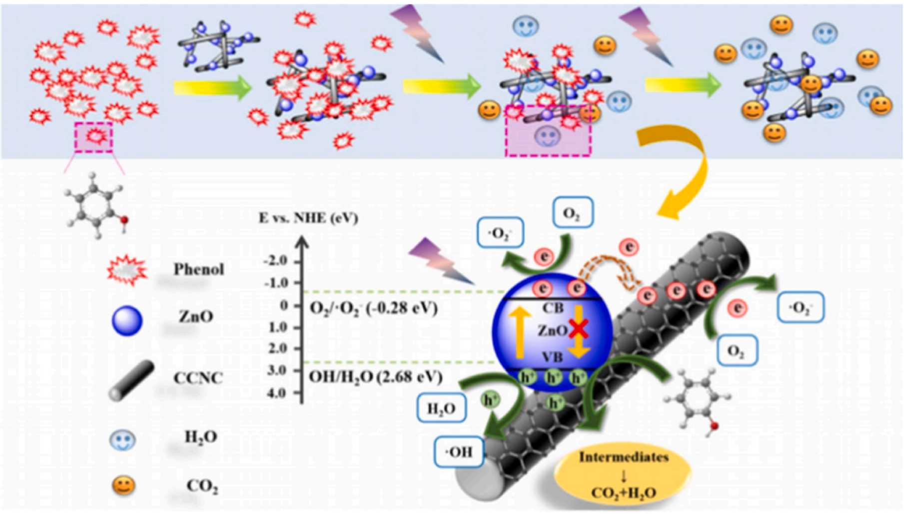

Fig. 7. Photocatalytic degradation process of phenol by ZnO-BC. Reproduced with permission from Zhang et al. [84].

6. Remediation of contaminants from soil

The soil due to its versatility makes it more prone to pollution. A large variety of pollutants can be found in the soil. Heavy metals such as lead, arsenic, nickel, chromium, and organic contaminants are among the pollutants found in the soil. For the protection of animals and human health in contaminated soils, immobilization measures are essential. The efficiency of immobilization and elimination of heavy metal and toxic pollutants in the soil are driven by multiple mechanisms.

6.1. *Remediation of heavy metals in soils*

The efficiency of the metal-biochar composite in soil restoration is widely reported. This efficiency results from the high adsorption of inorganic pollutants by the metal-biochar composite, which restores nutrients, and controls the bacterial activity, and soil biota. For example, Fan et al. [96] fabricated sawdust-derived biochar-loaded nano-scale zero-valent iron (nZVI) and a Fe_2O_3 mixture to boost the immobilization ability of As. As mobility in the soil decreased compared to pristine BC treatment. This may be because of the co-precipitation and adsorption as a result of amorphous FeOOH of nZVI on the BC surface. Gao et al. [97] then as well co-pyrolyzed rape straw and KH_2PO_4 mixture and synthesized a biochar composite that exhibited stupendous binding capability for three toxic heavy metals (Pb, Cu and Cd). Table 7 illustrates the performance of metal-biochar composites in soil remediation. For example, Shen et al. [60] prepared MgO-recovered biochar for lead immobilization and recorded an immobilization rate of 50.71 % related to cation-π interactions enhanced by precipitation reactions on the surface of the biochar composite. Qiao et al. [98] prepared an iron phosphate nanoparticle-modified biochar (CMC@BC@ $Fe_3(PO_4)_2$) for cadmium reduction in soil and reported that Cd bioaccessibility was reduced by 80 %. Lyu et al. [99] synthesized an iron-based biochar composite for the immobilization of hexavalent chromium in soil. They showed that reduction/precipitation are the main mechanisms linked to Cr (VI) immobilization. Su et al. [100] developed a nanoscale iron-modified biochar (nZVI@BC) for Cr (VI) immobilization and reported that the zero-valent iron in the biochar reduced Cr (VI) in the soil to $Cr(OH)_3$ for a removal rate of 100 %.

The immobilization mechanisms were postulated to include direct precipitation and complexation reactions between the heavy metals, phosphate, and –OH on the surface of the metal-biochar composite or could be indirectly related to the enhanced encapsulation of metal ions with an increase in pH and available soil phosphorus.

Table 7
Efficiency of metal-biochar composites in soil remediation.

Biochar composite	Studies	% Removal	References
MgO-Biochar	Lead immobilization in soil	50.71	[60]
CMC@BC@$Fe_3(PO_4)_2$	Cadmium reduction in soil	80.00	[98]
CMC-FeS@	Chromium	94.70	[99]
nZVI@BC	immobilization in soil	100	[100]
nZVI/BC	Arsenic immobilization in soil	93	[96]
Hydroxyapatite-Biochar	Immobilization of Cadmium and Lead in soil	87.80 and 92.90	[76]
	Immobilization of Cadmium and Lead the Chinese cabbage shoots	95.40 and 97.20	
Fe(II)-Biochar	Immobilization of Cadmium in wheat and rice grains	16 and 54	[101]
Fe(II)-Biochar	Immobilization of Arsenic in wheat and rice grains	48 and 44	
Iron-biochar composite	Immobilization of Cadmium and Arsenic in soil	36.40 and 24.80	[102]
Ferromanganese oxide biochar composites	Reduction in the concentration of arsenic in rice grains	78.30	[103]

6.2. *Remediation of organic and other pollutants in soils*

Adsorption, plaque formation and microbial stimulation are the main mechanisms by which metal-biochar composites immobilize organic adsorbates in soils. For example, Tan et al. [104] showed that the use of iron oxide-based biochar in soils leads to the formation of an iron plaque, which is responsible for the reduction of the pesticide chlorpyrifos. Heo et al. [105] reported that hydrogen bonding and π-π interactions controlled the binding of bisphenol and sulfamethoxazole to $CuZnFe_2O_4$-loaded biochar in soil. Furthermore, Fen et al. [106] showed that Nano-Ce_2O functionalized biochar (Ce-MSB) can retain 22.33 % of phosphate in soil via chemisorption. Riddle et al. [107] reported the efficiency of a magnesium (hydrous) oxide-coated biochar to bind 75 % of phosphate in soil. Oleszczuk et al. [108] prepared a zero iron nanoparticle-modified biochar for the degradation of polycyclic aromatic hydrocarbons (PAHs) in soil. They reported that nZVI-BC had the same sequestration properties as pristine BC for a degradation rate of 82 % of PAHs. Fig. 8 is a pictorial representation of a detailed mechanism for the sequestration of toxic pollutants using a metal biochar composite.

7. Limitation of the metal-biochar composite

Metal-biochar composites, because of their combined properties, are novel materials for solving environmental pollution. Nevertheless, these composites are not without inherent limitations and challenges, which include.

i The synthesis method, regeneration method and identity of the metal and biochar source all affect the textural properties, surface functions, and efficiency in immobilizing pollutants and presently may be difficult to determine *a priori.* Machine learning may be employed to better predict the dependence of the properties on the aforementioned variables.

ii Applications of metal-biochar composites can lead to leaching of metals present on the surface of biochar into the environment and consequently cause secondary pollution and toxicity to wildlife [40,64,109]. Thus, the innovation of more "green" synthesis and manufacturing methods is necessary. The use of more toxic metal ions should be discouraged.

iii The utilization of metal-biochar amalgam to ameliorate soil properties and for immobilization contaminants can have a significant short- and long-term influence on the aggregation, surface potential, pH and density of soils. Control of these physicochemical characteristics should be monitored during application.

iv The production of metal-biochar composite requires kilns where the temperatures need to be maintained at 400–700 °C for several hours, generating carbon gases and a lot of thermal energy. Recovery of gas emissions is necessary to reduce carbon footprint in the environment.

vii The use of metal biochar composites in soil can generate genotoxicity in ground glass due to the increase in pH at high metal concentrations in the soil.

Although the advantageous properties and durability of these biochar-based composites have already been addressed and discussed, the cost of production of these must also be taken into account before implementation at an industrial scale.

8. Future perspectives

This review paper noted the need for extended research on the development of improved and green synthetic routes for metal-biochar-loaded waste and their use in the fight against pollution. Studies on life cycle assessment (LCA) of metal-biochar composites, cost analysis, pilot-scale studies, and health and environmental risks are also critically needed for a comprehensive view of the subject for practical application. LCA allows for assessment of the feasibility and sustainability of metal-biochar composites for application in industrial scale or field application, and unforeseen challenges unpredicted from laboratory-scale studies. Machine learning studies are required to predict and optimize the properties of metal-biochar composites and their performance to save on synthesis costs and to better understand their chemistry using the existing literature. A similar approach has been used for other adsorbents [110].

9. Conclusions

This review provides a succinct critique and summary of the preparation and utilization of metal and metal oxide decorated biochar composites for the effective sequestration of various environmental contaminants from soil and wastewater and the interaction mechanisms involved. The role of metal-biochar composite is to provide reliable and sustainable approaches for dealing with traditional and emerging contaminants. Metal-biochar composites are promising novel materials for the efficient sequestration of noxious contaminants from environmental compartments such as soil and water. The known problem is the potential release of fine particles into the environment during the application of metal-biochar composites, causing biological toxicity among other human health risks. Therefore, it is important to explore the development of more green synthesis and fabrication methods and monitor the fate of the metal ions. Although biomass or feedstock for biochar is readily available, the overall cost of production could be relatively high, because of factors such as synthesis materials and energy

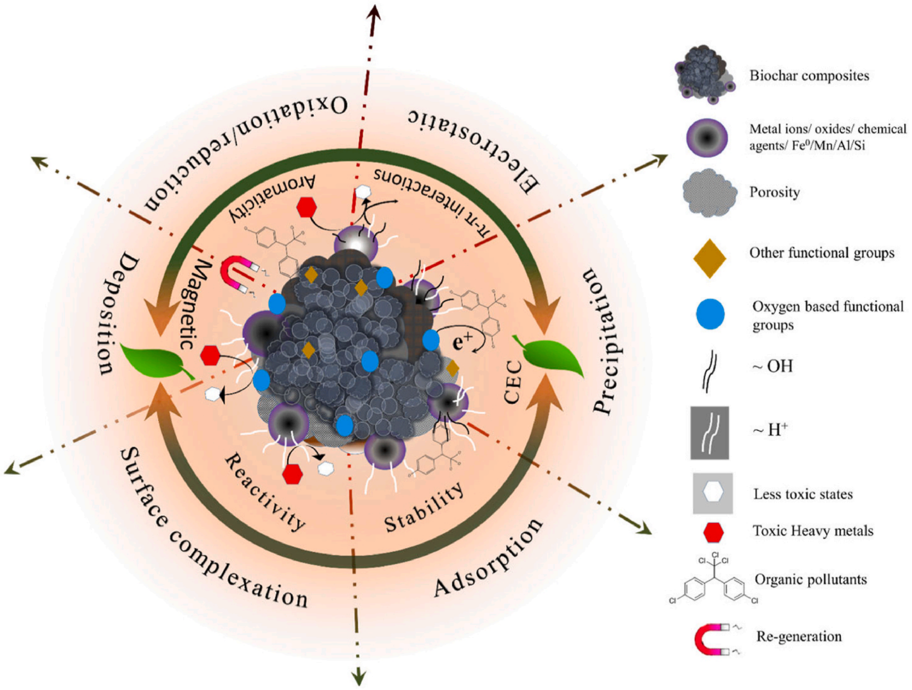

Fig. 8. Properties and removal processes of toxic pollutants from soils using metal-biochar composites. Reproduced with permission from Mandal et al. [22].

for pyrolysis.

Funding

No funding was received for this research.

Data availability

No data was generated in the development of this manuscript.

CRediT authorship contribution statement

Hermann Tamaguelon Dzoujo: Writing – original draft, Methodology. **Victor Odhiambo Shikuku:** Writing – review & editing, Conceptualization. **Sylvain Tome:** Writing – original draft, Investigation. **Aurelle Clandy Ntinkam Simo:** Writing – review & editing. **Emily C. Ng'eno:** Writing – original draft. **Zachary M. Getenga:** Writing – review & editing. **Marie Annie Etoh:** Writing – review & editing. **David Daniel Joh Dina:** Writing – review & editing.

Declaration of competing interest

The authors declare that they have no known competing financial interests or personal relationships that could have appeared to influence the work reported in this paper.

References

[1] P. Bottoni, S. Caroli, A.B. Caracciolo, Pharmaceuticals as priority water contaminants, Toxicol. Environ. Chem. 92 (2010) 549–565, https://doi.org/10.1080/02772241003614320.

[2] M. Yang, A current global view of environmental and occupational cancers, Journal of Environmental Science and Health - Part C Environmental Carcinogenesis and Ecotoxicology Reviews 29 (2011) 223–249, https://doi.org/10.1080/10590501.2011.601848.

[3] E.C. Ngeno, K.E. Mbuci, M.C. Necibi, V.O. Shikuku, C. Olisah, R. Ongulu, H. Matovu, P. Ssebugere, A. Abushaban, M. Sillanpä, Sustainable re-utilization of waste materials as adsorbents for water and wastewater treatment in Africa: recent studies, research gaps, and way forward for emerging economies, Environmental Advances 9 (2022) 100282, https://doi.org/10.1016/j.envadv.2022.100282.

[4] Y.J. Jo, E.Y. Choi, N.W. Choi, C.K. Kim, Antibacterial and hydrophilic characteristics of poly(ether sulfone) composite membranes containing zinc oxide nanoparticles grafted with hydrophilic polymers, Ind. Eng. Chem. Res. 55 (2016) 7801–7809, https://doi.org/10.1021/acs.iecr.6b01510.

[5] J.M. Mboka, H.D. Tamaguelon, V. Shikuku, S. Tome, V.F. Deugueu, H. Othman, et al., Novel superadsorbent from pozzolan-charcoal based geopolymer composite for the efficient removal of aqueous crystal violet, Water Air Soil Pollut. 235 (2024) 1–17, https://doi.org/10.1007/s11270-024-07257-4.

[6] H. Dzoujo, V. Odhiambo, S. Tome, F. Gallo, P. Ondiek, T. Strothmann, et al., Unary adsorption of sulfonamide antibiotics onto pozzolan-tyre ash based geopolymers : isotherms, kinetics and mechanisms, Chem. Eng. Res. Des. 206 (2024) 440–452, https://doi.org/10.1016/j.cherd.2024.05.009.

[7] S. Tome, H. Dzoujo, V. Shikuku, A. Nana, M. Annie, C. Rüscher, et al., Elimination of malachite green from aqueous and saline water by laterite-derived Na-polyferrosialate and polyferrophosphosialate geopolymers : a comparative study, Ceram. Int. (2023), https://doi.org/10.1016/j.ceramint.2023.11.252.

[8] V.O. Shikuku, S. Tome, D.T. Hermann, G.A. Tompsett, M.T. Timko, Rapid adsorption of cationic methylene blue dye onto volcanic ash - metakaolin based geopolymers, Silicon 14 (2022) 9349–9359, https://doi.org/10.1007/s12633-021-01637-9.

[9] H. Dzoujo Tamaguelon, V.O. Shikuku, S. Tome, S. Akiri, N.M. Kengne, S. Abdpour, et al., Synthesis of pozzolan and sugarcane bagasse derived geopolymer-biochar composites for methylene blue sequestration from aqueous medium, J. Environ. Manag. 318 (2022) 115533, https://doi.org/10.1016/j.jenvman.2022.115533.

[10] E.C. Ngeno, V.O. Shikuku, F. Orata, L.D. Baraza, S.J. Kimosop, Caffeine and ciprofloxacin adsorption from water onto clinoptilolite: linear isotherms, kinetics, thermodynamic and mechanistic studies, S. Afr. J. Chem. 72 (2019) 136–142, https://doi.org/10.17159/0379-4350/2019/V72A17.

[11] V.O. Shikuku, T. Mishra, Adsorption isotherm modeling for methylene blue removal onto magnetic kaolinite clay: a comparison of two-parameter isotherms, Appl. Water Sci. 11 (2021) 1–9, https://doi.org/10.1007/s13201-021-01440-2.

[12] T. Chimi, B.U. Hannah, N.M. Lincold, M.B. Jacques, S. Tome, D.T. Hermann, et al., Preparation, characterization and application of H3PO4 - activated carbon from Pentaclethra macrophylla pods for the removal of Cr (VI) in aqueous medium, J. Iran. Chem. Soc. (2022), https://doi.org/10.1007/s13738-022-02675-9.

[13] M.B. Jacques, N.P. Guy, M.L. Jules, Z.P. Harlette, M.E. Judith, M. Said, et al., Removal of crystal violet by TiO 2 loaded alkali-activated carbon hybrid material from Raphia farinifera fruit kernels : surface chemistry, parameters and mechanisms, Biomass Conversion and Biorefinery (2023) 1–21, https://doi.org/10.1007/s13399-023-04988-y.

[14] S. Jemutai-Kimosop, F. Orata, V.O. Shikuku, V.A. Okello, Z.M. Getenga, Insights on adsorption of carbamazepine onto iron oxide modified diatomaceous earth: kinetics, isotherms, thermodynamics, and mechanisms, Environ. Res. 180 (2020) 108898, https://doi.org/10.1016/J.ENVRES.2019.108898.

[15] V.O. Shikuku, S. Jemutai-kimosop, Efficient removal of sulfamethoxazole onto sugarcane bagasse-derived biochar : two and three-parameter isotherms, kinetics and thermodynamics, S. Afr. J. Chem. 111–9 (2020), https://doi.org/10.17159/0379-4350/2020/v73a16.

[16] G. Achieng, V. Shikuku, Adsorption of copper ions from water onto fish scales derived biochar: isothermal perspectives, J. Mater. Environ. Sci. 2020 (2020) 1816–1827.

[17] K.S.D. Premarathna, A.U. Rajapaksha, B. Sarkar, E.E. Kwon, A. Bhatnagar, Y. S. Ok, et al., Biochar-based engineered composites for sorptive decontamination of water: a review, Chem. Eng. J. 372 (2019) 536–550, https://doi.org/10.1016/J.CEJ.2019.04.097.

[18] B. Sajjadi, J.W. Broome, W.Y. Chen, D.L. Mattern, N.O. Egiebor, N. Hammer, et al., Urea functionalization of ultrasound-treated biochar: a feasible strategy for enhancing heavy metal adsorption capacity, Ultrason. Sonochem. 51 (2019) 20–30, https://doi.org/10.1016/j.ultsonch.2018.09.015.

[19] E. Weidner, E. Karbassiyazdi, A. Altaee, T. Jesionowski, F. Ciesielczyk, Hybrid metal oxide/biochar materials for wastewater treatment technology: a review, ACS Omega 7 (2022) 27062–27078, https://doi.org/10.1021/acsomega.2c02909.

[20] L. Liang, F. Xi, W. Tan, X. Meng, B. Hu, X. Wang, Review of organic and inorganic pollutants removal by biochar and biochar-based composites, Biochar 3 (2021) 255–281, https://doi.org/10.1007/s42773-021-00101-6.

[21] F.U. Haider, J.A. Coulter, L. Cai, S. Hussain, S.A. Cheema, J. Wu, et al., An overview of biochar production, its implications, and mechanisms of biochar-induced amelioration of soil and plant characteristics, Pedosphere 32 (2022) 107–130, https://doi.org/10.1016/S1002-0160(20)60094-7.

[22] S. Mandal, S. Pu, S. Adhikari, H. Ma, D. Kim, Technology Progress and future prospects in biochar composites : application and reflection in the soil environment, Crit. Rev. Environ. Sci. Technol. 0 (2020) 1–53, https://doi.org/10.1080/10643389.2020.1713030.

[23] J. Zhang, D. Hou, Z. Shen, F. Jin, D. O'Connor, S. Pan, et al., Effects of excessive impregnation, magnesium content, and pyrolysis temperature on MgO-coated watermelon rind biochar and its lead removal capacity, Environ. Res. 183 (2020) 109152, https://doi.org/10.1016/J.ENVRES.2020.109152.

[24] L. Wang, Y. Wang, F. Ma, V. Tankpa, S. Bai, X. Guo, et al., Mechanisms and reutilization of modified biochar used for removal of heavy metals from wastewater: a review, Sci. Total Environ. 668 (2019) 1298–1309, https://doi.org/10.1016/J.SCITOTENV.2019.03.011.

[25] S. Yi, Y. Sun, X. Hu, H. Xu, B. Gao, Porous nano-cerium oxide wood chip biochar composites for aqueous levofloxacin removal and sorption mechanism insights, Environ. Sci. Pollut. Control Ser. (2017), https://doi.org/10.1007/s11356-016-8342-1.

[26] X. Tan, Y. Liu, G. Zeng, X. Wang, X. Hu, Y. Gu, Application of biochar for the removal of pollutants from aqueous solutions, Chemosphere 125 (2015) 70–85, https://doi.org/10.1016/j.chemosphere.2014.12.058.

[27] N.A.S. Mohammed, R.A. Abu-Zurayk, I. Hamadneh, A.H. Al-Dujaili, Phenol adsorption on biochar prepared from the pine fruit shells: equilibrium, kinetic and thermodynamics studies, J. Environ. Manag. 226 (2018) 377–385, https://doi.org/10.1016/J.JENVMAN.2018.08.033.

[28] K. Kameyama, T. Miyamoto, Y. Iwata, T. Shiono, Influences of feedstock and pyrolysis temperature on the nitrate adsorption of biochar, Soil Sci. Plant Nutr. 62 (2016) 180–184, https://doi.org/10.1080/00380768.2015.1136553.

[29] M. Uchimiya, L.H. Wartelle, K.T. Klasson, C.A. Fortier, M. Isabel, Influence of pyrolysis temperature on biochar property and function as a heavy metal sorbent in soil, J. Agric. Food Chem. (2011) 1–5, https://doi.org/10.1021/jf104206c.

[30] Q. Yuan, Y. He, B. Mao, P. Zuo, W. Wu, Y. Huang, et al., NanoImpact Nano-metal oxides naturally attenuate antibiotic resistance in wastewater : killing antibiotic resistant bacteria by dissolution and decreasing antibiotic tolerance by attachment, NanoImpact 18 (2020), https://doi.org/10.1016/j.impact.2020.100225.

[31] M. Ahmad, S.S. Lee, X. Dou, D. Mohan, J.K. Sung, J.E. Yang, et al., Effects of pyrolysis temperature on soybean stover- and peanut shell-derived biochar properties and TCE adsorption in water, Bioresour. Technol. 118 (2012) 536–544, https://doi.org/10.1016/J.BIORTECH.2012.05.042.

[32] P. Mohanty, S. Nanda, K.K. Pant, S. Naik, J.A. Kozinski, A.K. Dalai, Evaluation of the physiochemical development of biochars obtained from pyrolysis of wheat straw, timothy grass and pinewood: effects of heating rate, J. Anal. Appl. Pyrol. 104 (2013) 485–493, https://doi.org/10.1016/j.jaap.2013.05.022.

[33] T. Chen, Y. Zhang, H. Wang, W. Lu, Z. Zhou, Y. Zhang, et al., Influence of pyrolysis temperature on characteristics and heavy metal adsorptive performance of biochar derived from municipal sewage sludge, Bioresour. Technol. 164 (2014) 47–54, https://doi.org/10.1016/J.BIORTECH.2014.04.048.

[34] F.N.D. Mukome, X. Zhang, L.C.R. Silva, J. Six, S.J. Parikh, Use of chemical and physical characteristics to investigate trends in biochar feedstocks, J. Agric. Food Chem. 61 (2013) 2196–2204, https://doi.org/10.1021/jf3049142.

[35] Y. Li, J. Shao, X. Wang, Y. Deng, H. Yang, H. Chen, Characterization of modified biochars derived from bamboo pyrolysis and their utilization for target component (furfural) adsorption, Energy Fuel. 28 (2014) 5119–5127, https://doi.org/10.1021/ef500725c.

[36] W. Liu, K. Tian, H. Jiang, H. Yu, Harvest of Cu NP anchored magnetic carbon materials from Fe/Cu preloaded biomass : their, Green Chem. (2014) 4198–4205, https://doi.org/10.1039/c4gc00599f.

[37] A.W. Samsuri, F. Sadegh-Zadeh, B.J. Seh-Bardan, Adsorption of As(III) and As(V) by Fe-coated biochars and biochars produced from empty fruit bunch and rice husk, J. Environ. Chem. Eng. 1 (2013) 981–988, https://doi.org/10.1016/J.JECE.2013.08.009.

[38] Z. Song, F. Lian, Z. Yu, L. Zhu, B. Xing, W. Qiu, Synthesis and characterization of a novel MnOx-loaded biochar and its adsorption properties for Cu2+ in aqueous solution, Chem. Eng. J. 242 (2014) 36–42, https://doi.org/10.1016/J.CEJ.2013.12.061.

[39] K. Xu, F. Lin, X. Dou, M. Zheng, W. Tan, C. Wang, Recovery of ammonium and phosphate from urine as value-added fertilizer using wood waste biochar loaded with magnesium oxides, J. Clean. Prod. 187 (2018) 205–214, https://doi.org/10.1016/J.JCLEPRO.2018.03.206.

[40] L. Lu, R. Shan, Y. Shi, S. Wang, H. Yuan, A novel TiO2/biochar composite catalyst for photocatalytic degradation of methyl orange, Chemosphere 222 (2019) 391–398, https://doi.org/10.1016/J.CHEMOSPHERE.2019.01.132.

[41] L. Long, Y. Xue, Y. Zeng, K. Yang, C. Lin, Synthesis, characterization and mechanism analysis of modified crayfish shell biochar possessed ZnO nanoparticles to remove trichloroacetic acid, J. Clean. Prod. 166 (2017) 1244–1252, https://doi.org/10.1016/J.JCLEPRO.2017.08.122.

[42] A. Khataee, B. Kayan, P. Gholami, D. Kalderis, S. Akay, L. Dinpazhoh, Sonocatalytic degradation of Reactive Yellow 39 using synthesized ZrO2 nanoparticles on biochar, Ultrason. Sonochem. 39 (2017) 540–549, https://doi.org/10.1016/J.ULTSONCH.2017.05.023.

[43] A. Khataee, P. Gholami, D. Kalderis, E. Pachatouridou, M. Konsolakis, Preparation of novel CeO2-biochar nanocomposite for sonocatalytic degradation of a textile dye, Ultrason. Sonochem. 41 (2018) 503–513, https://doi.org/10.1016/J.ULTSONCH.2017.10.013.

[44] D. Mohan, P. Singh, A. Sarswat, P.H. Steele, C.U. Pittman, Lead sorptive removal using magnetic and nonmagnetic fast pyrolysis energy cane biochars, J. Colloid Interface Sci. 448 (2015) 238–250, https://doi.org/10.1016/j.jcis.2014.12.030.

[45] N. Chaukura, E.C. Murimba, W. Gwenzi, Synthesis, characterisation and methyl orange adsorption capacity of ferric oxide – biochar nano-composites derived from pulp and paper sludge, Appl. Water Sci. (2016), https://doi.org/10.1007/s13201-016-0392-5.

[46] Y. Han, X. Cao, X. Ouyang, S.P. Sohi, J. Chen, Adsorption kinetics of magnetic biochar derived from peanut hull on removal of Cr (VI) from aqueous solution: effects of production conditions and particle size, Chemosphere 145 (2016) 336–341, https://doi.org/10.1016/j.chemosphere.2015.11.050.

[47] D. Mohan, H. Kumar, A. Sarswat, M. Alexandre-Franco, C.U. Pittman, Cadmium and lead remediation using magnetic oak wood and oak bark fast pyrolysis biochars, Chem. Eng. J. 236 (2014) 513–528, https://doi.org/10.1016/j.cej.2013.09.057.

[48] H. Lyu, B. Gao, F. He, A.R. Zimmerman, C. Ding, H. Huang, et al., Effects of ball milling on the physicochemical and sorptive properties of biochar : experimental observations and governing mechanisms, Environmental Pollution 233 (2018) 54–63, https://doi.org/10.1016/j.envpol.2017.10.037.

[49] K.W. Jung, S.Y. Lee, Y.J. Lee, Facile one-pot hydrothermal synthesis of cubic spinel-type manganese ferrite/biochar composites for environmental remediation of heavy metals from aqueous solutions, Bioresour. Technol. 261 (2018) 1–9, https://doi.org/10.1016/J.BIORTECH.2018.04.003.

[50] H. Dong, J. Deng, Y. Xie, C. Zhang, Z. Jiang, Y. Cheng, et al., Stabilization of Nanoscale Zero-Valent Iron (nZVI) with Modified Biochar for Cr(VI) Removal from Aqueous Solution, Elsevier B.V, 2017, https://doi.org/10.1016/j.jhazmat.2017.03.002.

[51] Q. Huang, S. Song, Z. Chen, B. Hu, J. Chen, X. Wang, Biochar-based materials and their applications in removal of organic contaminants from wastewater : state-of-the-art review, Biochar 1 (2019) 45–73, https://doi.org/10.1007/s42773-019-00006-5.

[52] C. Zhao, B. Wang, B.K.G. Theng, P. Wu, F. Liu, S. Wang, et al., Formation and mechanisms of nano-metal oxide-biochar composites for pollutants removal : a review, Sci. Total Environ. 767 (2021) 145305, https://doi.org/10.1016/j.scitotenv.2021.145305.

[53] M.C. Wang, G.D. Sheng, Y.P. Qiu, A novel manganese-oxide/biochar composite for efficient removal of lead(II) from aqueous solutions, Int. J. Environ. Sci. Technol. 12 (2015) 1719–1726, https://doi.org/10.1007/s13762-014-0538-7.

[54] K. Vijayaraghavan, Recent advancements in biochar preparation, feedstocks, modification, characterization and future applications, Environmental Technology Reviews 8 (2019) 47–64, https://doi.org/10.1080/21622515.2019.1631393.

[55] A.U. Rajapaksha, S.S. Chen, D.C.W. Tsang, M. Zhang, M. Vithanage, S. Mandal, et al., Engineered/designer biochar for contaminant removal/immobilization from soil and water: potential and implication of biochar modification, Chemosphere 148 (2016) 276–291, https://doi.org/10.1016/J.CHEMOSPHERE.2016.01.043.

[56] M. Lawrinenko, D. Jing, C. Banik, D.A. Laird, Aluminum and iron biomass pretreatment impacts on biochar anion exchange capacity, Carbon 118 (2017) 422–430, https://doi.org/10.1016/j.carbon.2017.03.056.

[57] Z. Yang, R. Xing, W. Zhou, L. Zhu, Adsorption characteristics of cipro fl oxacin onto g-MoS 2 coated biochar nanocomposites, Front. Environ. Sci. Eng. 14 (2020), https://doi.org/10.1007/s11783-019-1218-0.

[58] S. Kong, S. Loh, R. Thomas, S. Abdul, J. Salimon, Biochar from oil palm biomass : a review of its potential and challenges, Renew. Sustain. Energy Rev. 39 (2014) 729–739, https://doi.org/10.1016/j.rser.2014.07.107.

[59] C. Li, L. Zhang, Y. Gao, A. Li, Facile synthesis of nano ZnO/ZnS modified biochar by directly pyrolyzing of zinc contaminated corn stover for Pb (II), Cu (II) and Cr (VI) removals, Waste Management 79 (2018) 625–637, https://doi.org/10.1016/j.wasman.2018.08.035.

[60] Z. Shen, J. Zhang, D. Hou, D.C.W. Tsang, Y.S. Ok, D.S. Alessi, Synthesis of MgO-coated corncob biochar and its application in lead stabilization in a soil washing residue, Environ. Int. 122 (2019) 357–362, https://doi.org/10.1016/J.ENVINT.2018.11.045.

[61] Ronghua Li, Jim J. Wang, Baoyue Zhou, Mukesh Kumar Awasthia, Amjad Ali, Zengqiang Zhanga, A.M. Altaf Hussain Lahori, Recovery of phosphate from aqueous solution by magnesium oxide decorated magnetic biochar and its potential as phosphate-based fertilizer substitute, Bioresour. Technol. (2016), https://doi.org/10.1016/j.biortech.2016.02.125.

[62] R. Li, H. Deng, X. Zhang, J.J. Wang, M.K. Awasthi, Q. Wang, et al., High-efficiency removal of Pb(II) and humate by a CeO2–MoS2 hybrid magnetic biochar, Bioresour. Technol. 273 (2019) 335–340, https://doi.org/10.1016/j.biortech.2018.10.053.

[63] A.S. Eltaweil, Mohamed H. Ali, E.M. Abd El-Monaem, G.M. El-Subruiti, Mesoporous magnetic biochar composite for enhanced adsorption of malachite green dye: characterization, adsorption kinetics, thermodynamics and isotherms, Adv. Powder Technol. 31 (2020) 1253–1263, https://doi.org/10.1016/J.APT.2020.01.005.

[64] K. Zhang, J. Mao, B. Chen, Reconsideration of heterostructures of biochars: morphology, particle size, elemental composition, reactivity and toxicity, Environmental Pollution 254 (2019) 113017, https://doi.org/10.1016/j.envpol.2019.113017.

[65] J. Li, K. Zhang, H. Zhang, Adsorption of antibiotics on microplastics, Environmental Pollution 237 (2018) 460–467, https://doi.org/10.1016/j.envpol.2018.02.050.

[66] Y. Liu, S.P. Sohi, S. Liu, J. Guan, J. Zhou, J. Chen, Adsorption and reductive degradation of Cr(VI) and TCE by a simply synthesized zero valent iron magnetic biochar, J. Environ. Manag. 235 (2019) 276–281, https://doi.org/10.1016/j.jenvman.2019.01.045.

[67] K. Ioannou, P. Hadjiyiannis, I. Liatsou, I. Pashalidis, U(VI) adsorption by biochar fiber–MnO2 composites, J. Radioanal. Nucl. Chem. 320 (2019) 425–432, https://doi.org/10.1007/s10967-019-06479-9.

[68] Q. Zhou, B. Liao, L. Lin, W. Qiu, Z. Song, Adsorption of Cu(II) and Cd(II) from aqueous solutions by ferromanganese binary oxide–biochar composites, Sci. Total Environ. 615 (2018) 115–122, https://doi.org/10.1016/j.scitotenv.2017.09.220.

[69] Yu H. Faheem, J. Liu, J. Shen, X. Sun, J. Li, et al., Preparation of MnOx-loaded biochar for Pb2+ removal: adsorption performance and possible mechanism, J. Taiwan Inst. Chem. Eng. 66 (2016) 313–320, https://doi.org/10.1016/j.jtice.2016.07.010.

[70] M.I. Inyang, B. Gao, Y. Yao, Y. Xue, A. Zimmerman, A. Mosa, et al., A review of biochar as a low-cost adsorbent for aqueous heavy metal removal, Crit. Rev. Environ. Sci. Technol. 46 (2016) 406–433, https://doi.org/10.1080/10643389.2015.1096880.

[71] G. Tan, W. Sun, Y. Xu, H. Wang, N. Xu, Sorption of mercury (II) and atrazine by biochar, modified biochars and biochar based activated carbon in aqueous solution, Bioresour. Technol. 211 (2016) 727–735, https://doi.org/10.1016/j.biortech.2016.03.147.

[72] H. Zhang, R. Xiao, R. Li, A. Ali, A. Chen, Z. Zhang, Enhanced aqueous Cr(VI) removal using chitosan-modified magnetic biochars derived from bamboo residues, Chemosphere 261 (2020) 127694, https://doi.org/10.1016/j.chemosphere.2020.127694.

[73] M.R. Shang, Y.G. Liu, S.B. Liu, G.M. Zeng, X.F. Tan, L.H. Jiang, et al., A novel graphene oxide coated biochar composite: synthesis, characterization and application for Cr(VI) removal, RSC Adv. 6 (2016) 85202–85212, https://doi.org/10.1039/c6ra07151a.

[74] L. Yan, L. Kong, Z. Qu, L. Li, G. Shen, Magnetic biochar decorated with ZnS nanocrytals for Pb (II) removal, ACS Sustain. Chem. Eng. 3 (2015) 125–132, https://doi.org/10.1021/sc500619r.

[75] Z. Wu, X. Chen, B. Yuan, M.L. Fu, A facile foaming-polymerization strategy to prepare 3D MnO2 modified biochar-based porous hydrogels for efficient removal of Cd(II) and Pb(II), Chemosphere 239 (2020) 124745, https://doi.org/10.1016/J.CHEMOSPHERE.2019.124745.

[76] W. Wu, Z. Liu, M. Azeem, Z. Guo, R. Li, Y. Li, et al., Hydroxyapatite tailored hierarchical porous biochar composite immobilized Cd(II) and Pb(II) and mitigated their hazardous effects in contaminated water and soil, J. Hazard Mater. 437 (2022) 129330, https://doi.org/10.1016/J.JHAZMAT.2022.129330.

[77] T. Sun, Y. Sun, Y. Xu, L. Wang, X. Liang, Effective removal of Hg2+ and Cd2+ in aqueous systems by Fe–Mn oxide modified biochar: a combined experimental and DFT calculation, Desalination 549 (2023) 116306, https://doi.org/10.1016/J.DESAL.2022.116306.

[78] M. Luo, H. Lin, Y. He, B. Li, Y. Dong, L. Wang, Efficient simultaneous removal of cadmium and arsenic in aqueous solution by titanium-modified ultrasonic biochar, Bioresour. Technol. 284 (2019) 333–339, https://doi.org/10.1016/J.BIORTECH.2019.03.108.

[79] Hongmei Jin, Sergio Capareda, Zhizhou Chang, Jun Gao, Yueding Xu Jz, Biochar pyrolytically produced from municipal solid wastes for aqueous, Bioresource Technol 169 (2014) 622–629.

[80] J. Guo, C. Yan, Z. Luo, H. Fang, S. Hu, Y. Cao, Synthesis of a novel ternary HA/Fe-Mn oxides-loaded biochar composite and its application in cadmium(II) and

arsenic(V) adsorption, Journal of Environmental Sciences 85 (2019) 168–176, https://doi.org/10.1016/J.JES.2019.06.004.

[81] Y. Peng, M. Azeem, R. Li, L. Xing, Y. Li, Y. Zhang, et al., Zirconium hydroxide nanoparticle encapsulated magnetic biochar composite derived from rice residue: application for As(III) and As(V) polluted water purification, J. Hazard Mater. 423 (2022) 127081, https://doi.org/10.1016/J.JHAZMAT.2021.127081.

[82] J. Liu, B. Zhou, H. Zhang, J. Ma, B. Mu, W. Zhang, A novel Biochar modified by Chitosan-Fe/S for tetracycline adsorption and studies on site energy distribution, Bioresour. Technol. 294 (2019) 122152, https://doi.org/10.1016/j.biortech.2019.122152.

[83] P. Lisowski, J.C. Colmenares, O. Mašek, W. Lisowski, D. Lisovytskiy, A. Kamińska, et al., Dual functionality of TiO2/biochar hybrid materials: photocatalytic phenol degradation in the liquid phase and selective oxidation of methanol in the gas phase, ACS Sustain. Chem. Eng. 5 (2017) 6274–6287, https://doi.org/10.1021/acssuschemeng.7b01251.

[84] Y. Zhang, G. Zhao, Y. Xuan, L. Gan, M. Pan, Enhanced photocatalytic performance for phenol degradation using ZnO modified with nano-biochar derived from cellulose nanocrystals, Cellulose 28 (2021) 991–1009, https://doi.org/10.1007/s10570-020-03581-0.

[85] N.O. Rubangakene, M. Elkady, A. Elwardany, M. Fujii, H. Sekiguchi, H. Shokry, Effective decontamination of methylene blue from aqueous solutions using novel nano-magnetic biochar from green pea peels, Environ. Res. 220 (2023) 115272, https://doi.org/10.1016/J.ENVRES.2023.115272.

[86] L. Lu, R. Shan, Y. Shi, S. Wang, H. Yuan, A novel TiO2/biochar composite catalysts for photocatalytic degradation of methyl orange, Chemosphere 222 (2019) 391–398, https://doi.org/10.1016/j.chemosphere.2019.01.132.

[87] A. Khataee, B. Kayan, P. Gholami, D. Kalderis, S. Akay, Sonocatalytic degradation of an anthraquinone dye using TiO2-biochar nanocomposite, Ultrason. Sonochem. 39 (2017) 120–128, https://doi.org/10.1016/j.ultsonch.2017.04.018.

[88] D. Hao, Y. Chen, Y. Zhang, N. You, Nanocomposites of zero-valent iron@biochar derived from agricultural wastes for adsorptive removal of tetracyclines, Chemosphere 284 (2021) 131342, https://doi.org/10.1016/J.CHEMOSPHERE.2021.131342.

[89] Z. Chen, B. Lin, Y. Huang, Y. Liu, Y. Wu, R. Qu, et al., Pyrolysis temperature affects the physiochemical characteristics of lanthanum-modified biochar derived from orange peels: insights into the mechanisms of tetracycline adsorption by spectroscopic analysis and theoretical calculations, Sci. Total Environ. 862 (2023) 160860, https://doi.org/10.1016/J.SCITOTENV.2022.160860.

[90] Y. Hu, Y. Zhu, Y. Zhang, T. Lin, G. Zeng, S. Zhang, et al., An efficient adsorbent: simultaneous activated and magnetic ZnO doped biochar derived from camphor leaves for ciprofloxacin adsorption, Bioresour. Technol. 288 (2019) 121511, https://doi.org/10.1016/J.BIORTECH.2019.121511.

[91] R. Li, Z. Wang, X. Zhao, X. Li, X. Xie, Magnetic biochar-based manganese oxide composite for enhanced fluoroquinolone antibiotic removal from water, Environ. Sci. Pollut. Control Ser. 25 (2018) 31136–31148, https://doi.org/10.1007/s11356-018-3064-1.

[92] M.N. Hairuddin, N.M. Mubarak, M. Khalid, E.C. Abdullah, R. Walvekar, R. R. Karri, Magnetic palm kernel biochar potential route for phenol removal from wastewater, Environ. Sci. Pollut. Control Ser. 26 (2019) 35183–35197, https://doi.org/10.1007/s11356-019-06524-w.

[93] D. Zhang, Y. Li, S. Tong, X. Jiang, L. Wang, X. Sun, et al., Biochar supported sulfide-modified nanoscale zero-valent iron for the reduction of nitrobenzene, RSC Adv. 8 (2018) 22161–22168, https://doi.org/10.1039/c8ra04314k.

[94] S. Zhai, M. Li, D. Wang, L. Zhang, Y. Yang, S. Fu, In situ loading metal oxide particles on bio-chars: reusable materials for efficient removal of methylene blue from wastewater, J. Clean. Prod. 220 (2019) 460–474, https://doi.org/10.1016/J.JCLEPRO.2019.02.152.

[95] K.W. Jung, B.H. Choi, T.U. Jeong, K.H. Ahn, Facile synthesis of magnetic biochar/Fe3O4 nanocomposites using electro-magnetization technique and its application on the removal of acid orange 7 from aqueous media, Bioresour. Technol. 220 (2016) 672–676, https://doi.org/10.1016/J.BIORTECH.2016.09.035.

[96] J. Fan, X. Chen, Z. Xu, X. Xu, L. Zhao, H. Qiu, et al., One-pot synthesis of nZVI-embedded biochar for remediation of two mining arsenic-contaminated soils: arsenic immobilization associated with iron transformation, J. Hazard Mater. 398 (2020) 122901, https://doi.org/10.1016/j.jhazmat.2020.122901.

[97] R. Gao, H. Hu, Q. Fu, Z. Li, Z. Xing, U. Ali, et al., Remediation of Pb, Cd, and Cu contaminated soil by co-pyrolysis biochar derived from rape straw and orthophosphate: speciation transformation, risk evaluation and mechanism inquiry, Sci. Total Environ. 730 (2020) 139119, https://doi.org/10.1016/j.scitotenv.2020.139119.

[98] Y. Qiao, J. Wu, Y. Xu, Z. Fang, L. Zheng, W. Cheng, et al., Remediation of cadmium in soil by biochar-supported iron phosphate nanoparticles, Ecol. Eng. 106 (2017) 515–522, https://doi.org/10.1016/J.ECOLENG.2017.06.023.

[99] H. Lyu, H. Zhao, J. Tang, Y. Gong, Y. Huang, Q. Wu, et al., Immobilization of hexavalent chromium in contaminated soils using biochar supported nanoscale iron sulfide composite, Chemosphere 194 (2018) 360–369, https://doi.org/10.1016/J.CHEMOSPHERE.2017.11.182.

[100] H. Su, Z. Fang, P.E. Tsang, L. Zheng, W. Cheng, J. Fang, et al., Remediation of hexavalent chromium contaminated soil by biochar-supported zero-valent iron nanoparticles, J. Hazard Mater. 318 (2016) 533–540, https://doi.org/10.1016/J.JHAZMAT.2016.07.039.

[101] X. Tang, H. Shen, M. Chen, X. Yang, D. Yang, F. Wang, et al., Achieving the safe use of Cd- and As-contaminated agricultural land with an Fe-based biochar: a field study, Sci. Total Environ. 706 (2020) 135898, https://doi.org/10.1016/J.SCITOTENV.2019.135898.

[102] D. Pan, C. Liu, H. Yu, F. Li, A paddy field study of arsenic and cadmium pollution control by using iron-modified biochar and silica sol together, Environ. Sci. Pollut. Control Ser. 26 (2019) 24979–24987, https://doi.org/10.1007/s11356-019-05381-x.

[103] L. Lin, M. Gao, W. Qiu, D. Wang, Q. Huang, Z. Song, Reduced arsenic accumulation in indica rice (Oryza sativa L.) cultivar with ferromanganese oxide impregnated biochar composites amendments, Environmental Pollution 231 (2017) 479–486, https://doi.org/10.1016/J.ENVPOL.2017.08.001.

[104] X. Tang, J. Guo, Y. Yang, R. Tao, X. Feng, Use of Fe-impregnated biochar to efficiently sorb chlorpyrifos, reduce uptake by allium fi stulosum L. And enhance microbial community diversity, Agric Food Chem (2017) 5238–5243, https://doi.org/10.1021/acs.jafc.7b01300.

[105] J. Heo, Y. Yoon, G. Lee, Y. Kim, J. Han, C.M. Park, Enhanced adsorption of bisphenol A and sulfamethoxazole by a novel magnetic CuZnFe2O4–biochar composite, Bioresour. Technol. 281 (2019) 179–187, https://doi.org/10.1016/J.BIORTECH.2019.02.091.

[106] Y. Feng, H. Lu, Y. Liu, L. Xue, D.D. Dionysiou, L. Yang, et al., Nano-cerium oxide functionalized biochar for phosphate retention: preparation, optimization and rice paddy application, Chemosphere 185 (2017) 816–825, https://doi.org/10.1016/J.CHEMOSPHERE.2017.07.107.

[107] M. Riddle, L. Bergström, F. Schmieder, D. Lundberg, L. Condron, H. Cederlund, Impact of biochar coated with magnesium (hydr)oxide on phosphorus leaching from organic and mineral soils, J. Soils Sediments 19 (2019) 1875–1889, https://doi.org/10.1007/s11368-018-2197-7.

[108] P. Oleszczuk, M. Kołtowski, Effect of co-application of nano-zero valent iron and biochar on the total and freely dissolved polycyclic aromatic hydrocarbons removal and toxicity of contaminated soils, Chemosphere 168 (2017) 1467–1476, https://doi.org/10.1016/J.CHEMOSPHERE.2016.11.100.

[109] J. Liang, X. Li, Z. Yu, G. Zeng, Y. Luo, L. Jiang, et al., Amorphous MnO2 modified biochar derived from aerobically composted swine manure for adsorption of Pb (II) and Cd(II), ACS Sustain. Chem. Eng. 5 (2017) 5049–5058, https://doi.org/10.1021/acssuschemeng.7b00434.

[110] V.O. Shikuku, N. Masinde, Machine learning applications in adsorption of water pollutants, in: V. Shikuku (Ed.), Artificial Intelligence Applications in Water Treatment and Water Resource Management, IGI Global Publishers, 2023, pp. 1–30, https://doi.org/10.4018/978-1-6684-6791-6.ch001. ISBN13: 9781668467916.